Measuring Ground Reaction Force and Quantifying Variability in Jumping and Bobbing Actions

Madison G. McDonald[1] and Stana Živanović[2]

Abstract: This paper investigates variability in bobbing and jumping actions, including variations within a population of eight test subjects (intersubject variability) and variability on a cycle-by-cycle basis for each individual (intrasubject variability). A motion-capture system and a force plate were employed to characterize the peak ground reaction force, frequency of the activity, range of body movement, and dynamic loading factors for at least first three harmonics. In addition, contact ratios were also measured for jumping activity. It is confirmed that most parameters are frequency dependent and vary significantly between individuals. Moreover, the study provides a rare insight into intrasubject variations, revealing that it is more difficult to perform bobbing in a consistent way. The paper demonstrates that the vibration response of a structure is sensitive to cycle-by-cycle variations in the forcing parameters, with highest sensitivity to variations in the activity frequency. In addition, this paper investigates whether accurate monitoring of the ground reaction force is possible by recording the kinematics of a single point on the human body. It is concluded that monitoring the C7th vertebrae at the base of the neck is appropriate for recording frequency content of up to 4 Hz for bobbing and 5 Hz for jumping. The results from this study are expected to contribute to the development of stochastic models of human actions on assembly structures. The proposed simplified measurements of the forcing function have potential to be used for monitoring groups and crowds of people on structures that host sports and music events and characterizing human-structure and human-human interaction effects. **DOI: 10.1061/(ASCE)ST.1943-541X.0001649.**

Author keywords: Bobbing; Jumping; Variability; Ground reaction force; Body kinematics; Shock and vibratory effects.

Introduction

Vibration serviceability assessment under human-induced dynamic loading is one of the most challenging aspects of structural engineering design due to inherent randomness in frequency, duration, and type of human actions to which the structure could be exposed. Walking, running, rising up from sitting, sitting down from standing, swaying, jumping, and bobbing are frequently observed human activities that generate three-dimensional dynamic forces (Bachmann and Ammann 1987). This paper is concerned with two activities, rhythmic jumping and bobbing, which are of most interest in the design of stadia and concert venues (Jones et al. 2011b). Only the largest (i.e., vertical) component of the force, whose peak value could be up to seven times larger than the body weight (Bachmann and Ammann 1987), will be considered. The vertical force is often responsible for excessive vibrations that could lead to damage of nonstructural components, unwanted noise, discomfort, or panic among occupants, overstressing the structure, and, in rare cases, compromising the structural integrity.

The key difference between jumping and bobbing is that a jumping cycle consists of a contact and a flight phase, while bobbing can be seen as akin to an attempt to jump while maintaining continuous contact with the ground (Jones et al. 2011b). Distinctions are often made between two different styles of bobbing: bouncing and jouncing. Bouncing is a more controlled action during which heel contact is maintained with the ground at all times (Sim et al. 2005). In this case, the majority of the movement is caused by the subject bending their knees. Jouncing is a more energetic alterative in which the subject rises on to their toes, breaking contact between their heels and the floor (Jones et al. 2011b). The action of jouncing is more complex as maintaining balance while rising on to the toes requires the engagement of additional muscles and joints. While jumping is more severe in terms of loading amplitude (Ellis and Ji 1994), bobbing is more common at concerts and other events, as it requires less energy (and less space) to be maintained (Racic et al. 2013a; Dougill et al. 2006). In addition, bobbing is an important loading case as the person is more likely to feel the structural movement and potentially react, consciously or unconsciously, by synchronizing with it, which could lead to a prolonged and excessive vibration response.

Body kinematics while jumping and bobbing, as well as the resulting dynamic force, varies significantly within a human population. Moreover, a single individual produces different kinematic and kinetic outputs when performing nominally the same activity on different occasions, or even from one jumping/bobbing cycle to another (Sim et al. 2008; Racic and Pavic 2010a). Tackling limited understanding of dynamic loads with unnecessarily conservative and uneconomical designs is no longer acceptable in the age of performance-based design and expectation of minimum use of natural resources. Hence, modern design is somewhat contradictory: it favors structures that are lightweight and slender (and inherently vibration sensitive) while expecting vibration serviceable design solutions. Anticipating and preventing vibration serviceability failures requires detailed characterization of human actions and the intrinsic randomness in both the population and an individual's dynamic loading, neither of which is currently readily available to structural designers.

[1]Ph.D. Graduate, School of Engineering, Univ. of Warwick, Coventry CV4 7AL, U.K. E-mail: madison.mcdonald8@gmail.com

[2]Associate Professor, School of Engineering, Univ. of Warwick, Coventry CV4 7AL, U.K. (corresponding author). E-mail: s.zivanovic@warwick.ac.uk

Note. This manuscript was submitted on October 11, 2015; approved on July 15, 2016; published online on August 24, 2016. Discussion period open until January 24, 2017; separate discussions must be submitted for individual papers. This paper is part of the ***Journal of Structural Engineering***, © ASCE, ISSN 0733-9445.

Typically, jumping can be performed at frequencies between 1 and 4 Hz (Rainer et al. 1988; Pernica 1990). The peak value of the generated ground reaction force (GRF) is usually 2.0–4.5 times larger than the weight of the person jumping (Sim et al. 2008). This GRF results from trunk motion characterized by peak-to-peak displacements around 10–30 cm and acceleration around 15–35 m/s^2 (McDonald 2015). Bobbing can be performed at frequencies up to 6 Hz, albeit the upper limit of 4.0–5.0 Hz is more frequently encountered (Yao et al. 2004). Typical peak-to-peak trunk displacements while bobbing are about two times lower than while jumping as body movement is limited by the continuous contact with the ground. As a consequence, the GRF generated while bobbing is lower compared to jumping.

In design applications, the force is traditionally decomposed into the main harmonics using Fourier transform. The harmonics are then normalized by the body weight to calculate a dimensionless quantity called dynamic loading factor (DLF). For jumping, the upper limit of the DLF is typically 1.8 for the first, 1.0 for the second, and 0.3 for the third harmonic (Rainer et al. 1988), while the bobbing DLFs are typically about two times lower. The strength of the forcing harmonics normally reduces with an increase in harmonic frequency. As a result, the structures considered to be at risk from excessive vibrations are those with a natural frequency of up to 6 Hz (IStructE 2008). Accurate modeling of this low-frequency content of the force is considered to be most important for vibration serviceability assessment. Use of traditional models for this purpose has been found to be inadequate in vibration-prone structures as they cannot model the narrow band nature (i.e., randomness) of human-induced dynamic loading (Brownjohn et al. 2004).

Sim et al. (2008) were among first researchers to include cycle-by-cycle variations when modeling the force amplitude, contact time, and the frequency of people jumping. They proposed a cosine-squared function to represent each jumping cycle and therefore could not describe asymmetry and local irregularities in the forcing signal regularly encountered in measured data. Racic and Pavic (2010a) overcame these limitations by first modeling asymmetry in the force waveform as a sum of two Gaussian functions. They then extended their approach to a detailed modeling of local irregularities by utilizing a sufficiently large number of Gaussian functions and achieved excellent agreement (in both time domain and frequency domain) between simulated force waveforms and those seen in experiments (Racic and Pavic 2010b). Similar successful detailed modeling has been recently achieved for dynamic loading during bobbing (Racic and Chen 2015). These advanced studies, however, rarely report the degree of variability in parameters describing the jumping and bobbing forces and its influence on the structural response—the information that would be of direct interest to structural designers. Some modeling studies also rely on use of publically unavailable databases of measured force time histories to inform the choice of the modeling parameters. Providing direct insight into the variability of the individual parameters would contribute to bridging the gap between traditional deterministic modeling, featuring parameters with clear physical meaning, and more sophisticated and accurate, but also more complex, stochastic modeling approaches. This study aims to contribute towards characterizing variability in both jumping and bobbing actions and evaluating the importance of parameter variability for design. To achieve these aims, GRFs measured using a force plate will be utilized.

Another aim of this paper is to investigate the possibility of measuring the force in such a way as to overcome some limitations associated with other methods. Force plates are usually small (i.e., 400×600 or 600×600 mm) and normally limited to laboratory environments. The former makes targeting the landing area while jumping challenging, potentially leading to an unnatural jumping action that, in turn, affects the GRF waveform. Racic et al. (2013b) overcame these issues by utilizing a motion capture system. This system consists of a number of cameras that monitor either active or passive markers systematically attached to anatomical landmarks of the test subject's body, with the aim of recording the body kinematics during the observed activity. The GRF is then indirectly found by summing up the inertia forces of individual body segments (Thorton-Trump and Daher 1975; Racic et al. 2013b). This procedure, however, requires the use of a large number of markers, which may be logistically challenging, especially when monitoring several individuals simultaneously. Instead, it would be more convenient if the kinematics of the body center of mass (BCoM) could be directly measured. In this case, the acceleration of BCoM could be multiplied by the test subject's mass to derive the GRF. The challenge with this approach is that the BCoM is not directly accessible for monitoring as it is normally located within the test subject's trunk during jumping and bobbing. A potential solution is to identify a point on the human body whose kinematics closely resembles that of the BCoM. Identifying this point is the aim of the second part of this study.

The paper outline is as follows. The experimental procedure is described first. Then the variability in the jumping and bobbing actions is characterized. This is followed by the identification of a single point on the human body suitable for force measurement. Finally, the discussion and conclusions are presented.

Experimental Procedure

Experiments were conducted in the Gait Laboratory at the University of Warwick, Coventry, U.K. The laboratory is equipped with a Vicon (Oxford Metrics, Oxford, U.K.) motion capture system consisting of 12 infrared cameras (*Nexus*), two digital video cameras and a force plate OR6-7-2000 (AMTI 2007). Eight test subjects (TSs), four males and four females, volunteered to take part in the experiments. Their basic anthropometric properties are presented in Table 1. The TSs were instrumented with 17 reflective markers, positioned at locations with the potential to represent the movement of the BCoM well (Fig. 1). The markers were attached using double-sided tape. The TSs wore tight clothes as well as a muscle wrap around the lower trunk [highlighted in Fig. 1(d)] to minimize soft tissue artefacts, i.e., relative displacement between the markers and underlying bones (Racic et al. 2013b).

Six markers were placed on a TS's back: B1, B2, and B3 on the L5th, L3rd, and L1st vertebrae on the lower back, respectively, B4 on the T11th vertebrae, B5 on the T6th vertebrae on the middle back, i.e., between shoulder blades, and B6 on the C7th vertebrae at the base of the neck. Four markers were positioned on the hips: RH1 and LH1 on the anterior superior iliac spine on the right and left hip, respectively, while RH2 and LH2 were attached at the position of the greater trochanter on the right and left hip, respectively (Fig. 1). Seven markers were placed on the front of the TS (F1-F7 in Fig. 1) and spaced evenly up the torso. The majority of the markers

Table 1. Test Subject Data

	Test Subject							
Trait	1	2	3	4	5	6	7	8
Gender	M	F	M	F	F	M	M	F
Body mass (kg)	83	70	83	65	66	85	73	68
Height (m)	1.85	1.82	1.80	1.76	1.74	1.71	1.76	1.66

Note: F = Female; M = Male.

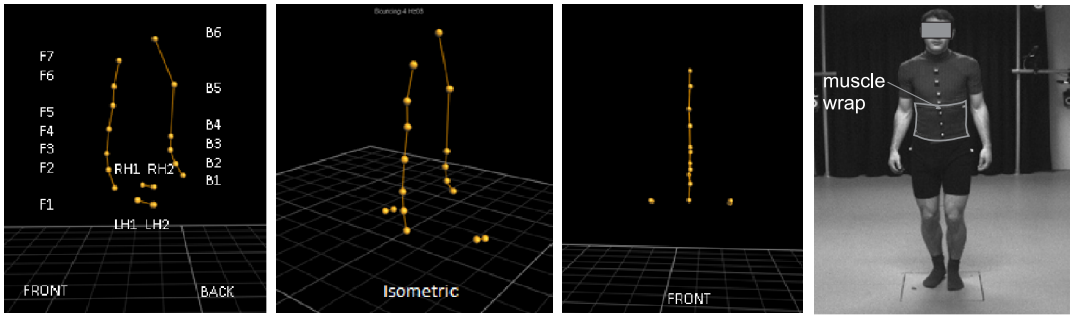

Fig. 1. (a) Side; (b) isometric; (c) frontal views of the 17 markers displayed using *Nexus*; B, H, and F stand for back, hip, and frontal markers; L and R stand for left and right; (d) frontal view of a test subject

were placed on the trunk as the BCoM locations for jumping and bobbing postures are known to be within this part of the human body.

The TSs were first asked to jump on the force plate at metronome-controlled frequencies of 1, 2, and 3 Hz. The frequency range was chosen to expose TSs to a wide range of jumping styles: extremely slow jumping (1 Hz) and relatively fast jumping (3 Hz) as well as comfortable jumping at 2 Hz (Yao et al. 2006). The frequency of 2 Hz was also chosen as it is often embedded in pop music (Ginty et al. 2001) acting as an aural stimulus for crowd actions at concert venues. After completion of these experiments, TSs performed bobbing at 1, 2, 3, and 4 Hz. The frequencies of 1–3 Hz were chosen to enable a comparison between bobbing and jumping activities at nominally the same frequencies, while the frequency of 4 Hz was added to reflect the ability of TSs to bob at frequencies above 3 Hz. Before each trial, the TSs were given enough time to familiarize themselves with the metronome beat and the test procedure, which was followed by 20 s of data collection. Between successive trials the TSs were given a few minutes to rest. During this break, the attachment of the markers was checked as were the force time histories, to ensure the TS did not miss the target force plate area. In rare cases when either of the two issues occurred, the previous trial was repeated. A test session with one TS, including preparation and briefing, lasted about 1 h.

Each trial consisted of simultaneous recording of the vertical component of the GRF (using the force plate) and the three-dimensional displacements of the markers (using the motion capture system). The force plate signal was sampled at 1,000 Hz while the marker displacements were recorded at 200 Hz. The high sampling rates (which were the maximum sampling rates available in the measurement systems) were chosen to ensure that the time step was sufficiently small, and therefore, the numerical errors negligible, in subsequent numerical time-domain simulations (Chopra 1995). All signals were filtered using a low-pass fifth order Butterworth filter in *MATLAB*. The cut-off frequency of the filter was 1 Hz above the frequency of the third forcing harmonic or 7 Hz, whichever was larger. This cut-off frequency was chosen to allow analysis of the first three harmonics that contain the most excitation energy, as well as all harmonics up to 6 Hz that have potential to strongly excite grandstand structures (IStructE 2008). The force plate signal was decimated to 200 Hz in those analysis cases requiring comparison with the marker signals. The 20-s-long signal consisted of 20–80 cycles, depending on the frequency of the activity. In total 24 trials of jumping and 32 trials of bobbing were recorded.

The experiments were approved by the Biomedical and Scientific Research Ethics Committee at the University of Warwick. The test protocol and health and safety details were explained to TSs initially in the recruitment phase, and then repeated just before the testing took place. Before commencing the tests, TSs completed a physical readiness questionnaire and signed a consent form. Only TSs with no known relevant health problems at the time of testing were allowed to take part in the experiments.

Characterizing Jumping and Bobbing

A typical time history of the low-pass-filtered force induced by jumping is shown in Fig. 2(a). Period T_i, contact time CT_i, and

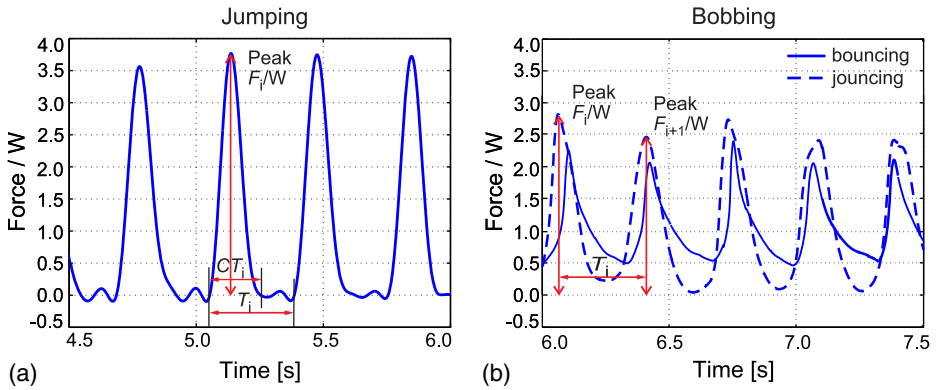

Fig. 2. Force generated at nominal frequency of 3 Hz for (a) jumping; (b) bobbing

Table 2. Bobbing Style at Different Frequencies for Eight Test Subjects

Frequency	TS1	TS2	TS3	TS4	TS5	TS6	TS7	TS8
1 Hz	J	J	J	B	B	J	B	J
2 Hz	B	J	J	B	J	J	B	J
3 Hz	B	J	J	B	J	J	J	J
4 Hz	J	J	J	B	J	B	J	J

Note: B = bouncing; J = jouncing.

peak force for the *i*th jumping cycle are denoted in the same figure. The force waveforms while bobbing are more diverse than those induced while jumping due to two distinct bobbing styles: bouncing and jouncing. Video footage of the TSs' heels was used to determine which style was preferred by each TS at each frequency. Table 2 shows that three TSs (TS2, TS3, and TS8) preferred the jouncing style while TS4 preferred to bounce at all four frequencies. The other four TSs made use of both styles, as a means of adapting to the imposed bobbing frequency. Interestingly, there is no correlation between the chosen style and the bobbing frequency across the population of four TSs. Overall, jouncing was encountered more frequently, i.e., in 22 out of 32 trials (69%). Fig. 2(b) shows bobbing force profiles at the nominal frequency of 3 Hz: the solid line represents TS1 bouncing while the dashed line depicts TS3 jouncing. The latter activity is usually more energetic resulting in a larger force compared with bouncing. In addition, the jouncing waveform can be similar to that of jumping, with troughs approaching zero (despite the fact that jouncing does not include a flight phase), as can be seen in the figure. However this observation cannot be generalized as low-energy jouncing and high-energy bouncing can also occur.

In the remainder of this section, the intersubject and/or intrasubject variations in the frequency, BCoM displacement, peak force, and DLFs for jumping and bobbing are shown and compared. Then the contact time, a parameter typical of jumping activity, is presented. At the end of the section, the vibration response is calculated and its sensitivity to randomness in the force investigated.

Parameters were extracted on a cycle-by-cycle basis to calculate the average value and the coefficient of variation (CoV) for each time history. To describe variability in the two statistical parameters (average and CoV) across the population of eight test subjects, their mean and standard deviation (SD) were also determined.

Activity Frequency

The frequency of each jump/bob cycle is calculated as the reciprocal value of the period T denoted in Fig. 2. The (actual) average frequency of each TS is plotted against the target frequency in Fig. 3(a), while the CoV is shown against the (actual) average frequency in Fig. 3(b). Similar information is shown in Figs. 3(c and d) for bobbing. The overall mean and the mean ± 1 SD from the population of eight TSs are presented as solid lines and dashed lines, respectively. Star and triangular symbols are used to distinguish between male and female TSs, while solid and hollow symbols [in Figs. 3(c and d)] denote jouncing and bouncing styles of bobbing, respectively.

Figs. 3(a and c) demonstrate that, when the average frequency value of each trial is considered, TSs were most successful in matching the slow frequency of 1 Hz for both jumping and bobbing actions. For all other beat frequencies, the difference between the target and the actual values was larger, with both overestimations (up to 21%) and underestimations (up to 14%) of the target frequency possible. While test subjects seem best able to target the

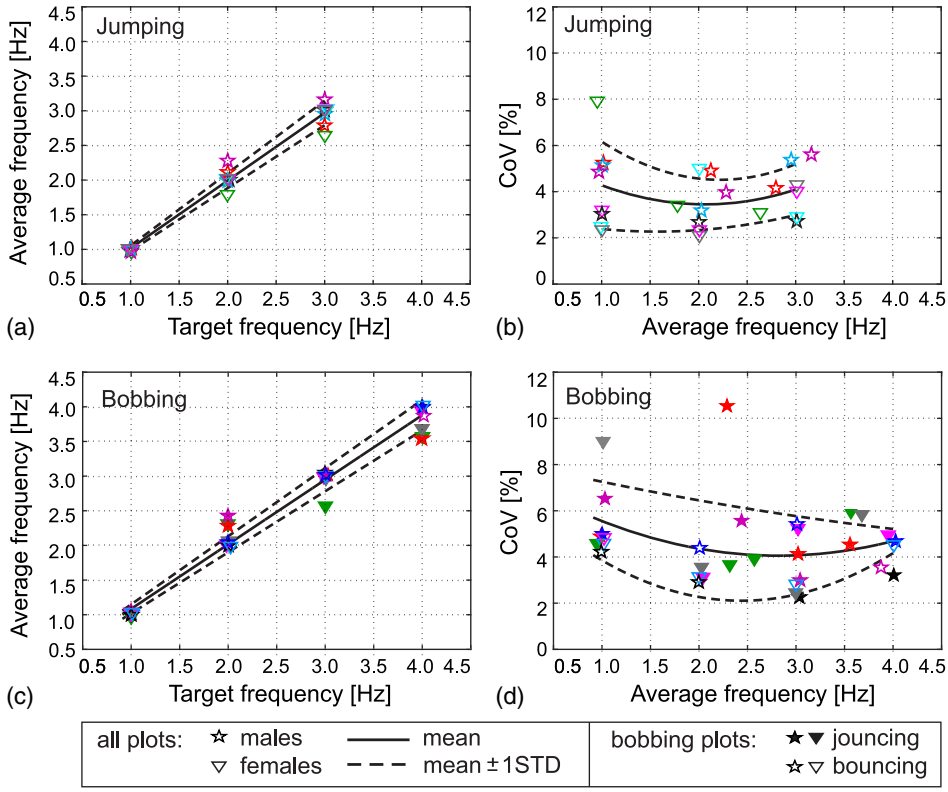

Fig. 3. (a) Average frequency as a function of the target frequency of jumping; (b) CoV as a function of the average frequency of jumping; (c) average frequency as a function of the target frequency of bobbing; (d) CoV as a function of the average frequency of bobbing

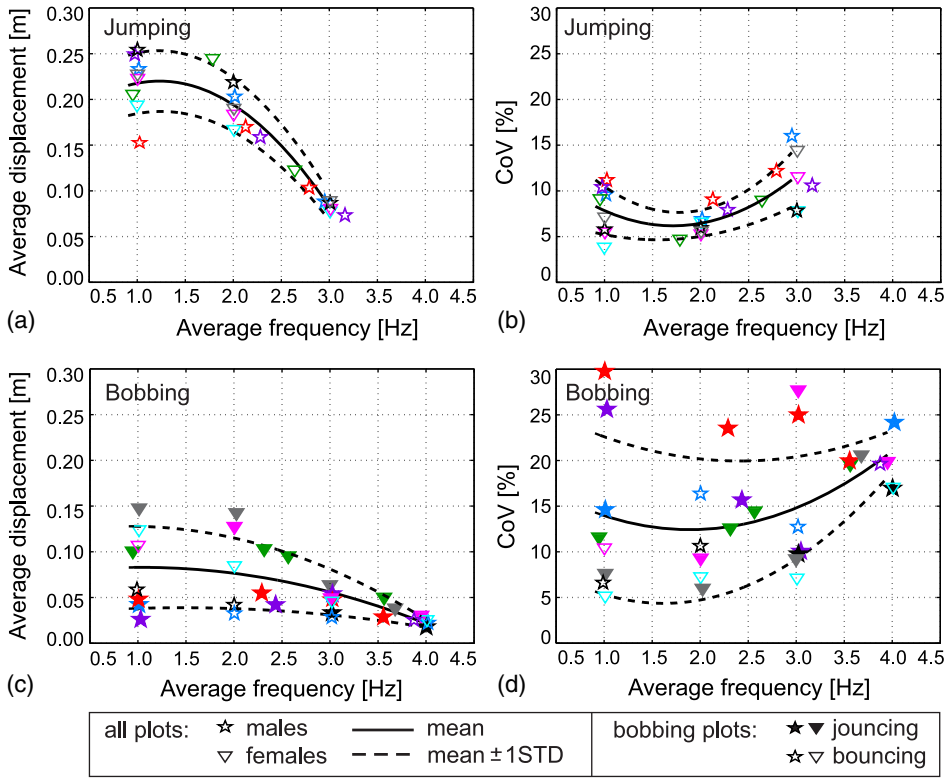

Fig. 4. (a) BCoM displacement; (b) its CoV as functions of the average frequency of jumping; (c) BCoM displacement; (d) its CoV as functions of the average frequency of bobbing

slow frequency of 1 Hz (in terms of the average value of a trial), the achieved frequency varied on the cycle-by-cycle basis slightly more, on average, than at higher frequencies [Figs. 3(b and d)]. It can also be seen that the cycle-by-cycle variation is larger when bobbing [Fig. 3(d)] than when jumping [Fig. 3(b)], and that both are larger than the maximum CoV of 3% observed when walking at a normal speed (Dang and Živanović 2015).

For consistency, the template for data presentation used in Fig. 3 will also be utilized for the remaining parameters, whenever possible.

Body Center of Mass Kinematics

The peak-to-peak vertical displacement of each jumping/bobbing cycle was found using the measured displacement trajectory for the B6 marker, which is a good representation of BCoM kinematics (as shown later in the "Ground Reaction Force" section). The average peak-to-peak displacements decrease with an increase in the jumping frequency [Fig. 4(a)]. The CoV values exhibit a global minimum at the most comfortable activity rate around 2 Hz [Fig. 4(b)]. Similar conclusions can be drawn for bobbing [Figs. 4(c and d)]. The range of movement while jumping can be more than two times larger than during bobbing. Bobbing on a cycle-by-cycle basis is less consistent than jumping (i.e., the CoV for bobbing is consistently larger, with maximum value being 30% compared with 16% for jumping). It can also be seen that the range of movement is larger when jouncing, compared with bouncing, due to the breaking of contact between the heels and the ground [Fig. 4(c)]. Displacement also varies more while jouncing [Fig. 4(d)]. In addition, the female TSs seem to be more energetic than male TSs while bobbing, resulting in a wider peak-to-peak body displacement [Fig. 4(c)] and, at the same time, achieving a better consistency [Fig. 4(d)]. This pattern is not present for jumping.

Peak Force

The average peak forces, normalized by TSs' weight W, and their CoV for both jumping and bobbing are shown in Fig. 5. On average, the lowest forces occur at 1 Hz in both cases, as this is a slow, relatively mild action with respect to the dynamic force generated [Figs. 5(a and c)]. The force increases with increase in activity frequency. It reaches a maximum value at the most comfortable frequencies (2 Hz for jumping, and 3 Hz for bobbing), and then it starts to decrease slowly at faster, less-conformable, activity rates. It can be seen that the mean value of the peak force for jumping [Fig. 5(a)], which is a more vigorous activity, is about 1.6 times larger than that for bobbing [Fig. 5(c)] at the same frequency (average bobbing peak forces range between 1.3 and 2.5, compared to 2.4–4.0 while jumping). In general, the peak forces were larger from jouncing than from bouncing [Fig. 5(c)].

As in the case of the previous two parameters, the peak force on a cycle-by-cycle basis varies more while bobbing [Fig. 5(d)] than while jumping [Fig. 5(b)]. The only exception is jumping at 2 Hz producing not only the largest force but also the largest jump-by-jump variation, the latter due to ability of test subjects to vary jumping style at this comfortable frequency.

Dynamic Load Factors

The DLFs were calculated for the first three harmonics for activities performed at 2, 3, and 4 Hz. For jumping and bobbing at 1 Hz, the first six harmonics were analyzed as they all can cause resonance for structures with a natural frequency below 6 Hz (IStructE 2008). A fifth-order band-pass Butterworth filter was used to extract each

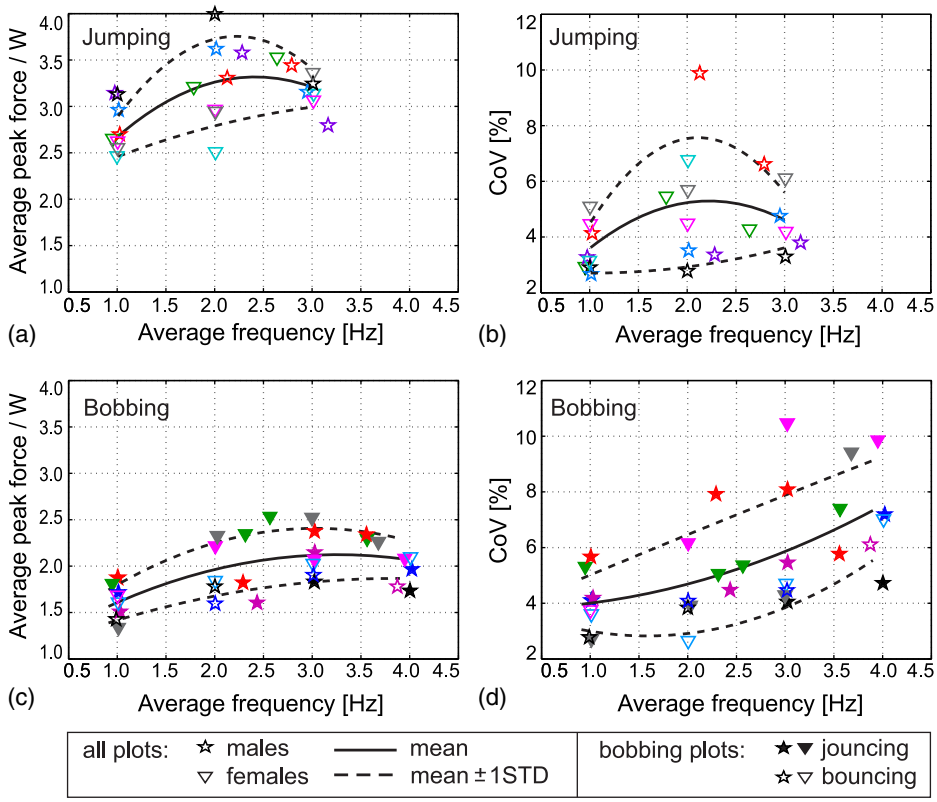

Fig. 5. (a) Normalized average peak force; (b) its CoV as functions of the average frequency of jumping; (c) normalized average peak force; (d) its CoV as functions of the average frequency of bobbing

harmonic on the average frequency ±3 SD bandwidth for the harmonic considered. The cycle-by-cycle amplitudes of the filtered force time histories were then found and their average value reported as a representative DLF value. Fig. 6 shows DLFs for each activity frequency. Large stars and triangles denote bobbing, while the small symbols denote jumping.

The DLFs for jumping at 1 Hz follow an unusual pattern [Fig. 6(a)], namely the first harmonic was smaller than the second, i.e., odd harmonics were lower than the even harmonics. This behavior is caused by time separation of the landing and launching actions, not present when jumping at quicker rates. It results in a double-peak force profile within a jumping cycle, causing the second harmonic (at 2 Hz), and more generally all even harmonics, to dominate. Consequently, separate relationships for even and odd harmonics are presented in Fig. 6(a). Bobbing at 1 Hz results in numerical values of DLFs that are generally lower than those values recorded for weaker (odd) harmonics caused by jumping at the same frequency. The DLF values for all three harmonics with respect to jumping at 2 Hz were similar to those due to jumping at 3 Hz and they decreased with increasing harmonic number [Figs. 6(b and c)]. In both cases the DLF values for bobbing were around two times lower. DLFs for bobbing at 4 Hz [Fig. 6(d)] are similar to those recorded while bobbing at 3 Hz.

Contact Ratio for Jumping

The contact ratio (i.e., contact time divided by period of the jumping cycle) is an important parameter that indicates the severity of the dynamic action. A shorter contact ratio implies a sharper force impact and therefore a larger dynamic force (Bachmann and Ammann 1987; BRE 2004). This inverse relationship between peak force and contact ratio for each jump is shown in Fig. 7(a). The figure also shows that jumping at a frequency of 3 Hz (black symbols), which is largest frequency used in this study, does not necessarily result in the shortest contact ratio, which is sometimes assumed in analytical force models (Bachmann and Ammann 1987). Fig. 7(b) reinforces this finding. In addition, it shows that the average contact ratio ranges from approximately 0.5 (at 2 Hz), to a large value of 0.8 (at extremely slow frequency of 1 Hz). There is a large variation in the contact ratio, especially for the frequency of 2 Hz. Fig. 7(c) shows that the jump-by-jump variability in the contact ratio, as well as the contact ratio scatter within the population of TSs, increases with increase in the frequency.

All the contact ratios observed in the tests were greater than 0.4 and 95.2% were above 0.5, similar to the findings of Sim et al. (2008) and Yao et al. (2002). A full 97.5% of contact ratios were greater than 0.72 for 1 Hz jumping, 0.46 for 2 Hz, and 0.51 for 3 Hz (McDonald 2015). Hence contact ratios that are lower than 0.5 are rare. These findings support Sim et al.'s statement that the contact ratios of 0.25–0.67, specified in the 1996 edition of British Standard (BS) 6399, underestimated the actual range of values. The updated version of this British standard issued in 2002 (BSI 2002) and its more recent Europewide successor (BSI 2010), do not include information on contact ratios, as an acknowledgement that further research and specialist guidance on its modeling are required.

Vibration Response

To get an insight into the actual vibration response potentially generated by an individual jumping or bobbing, the response of the structure, modeled as a single-degree-of-freedom (SDOF) system representing a relevant mode of vibration, to the measured force is presented in this section. In addition, sensitivity of the vibration response to the randomness in the force is evaluated.

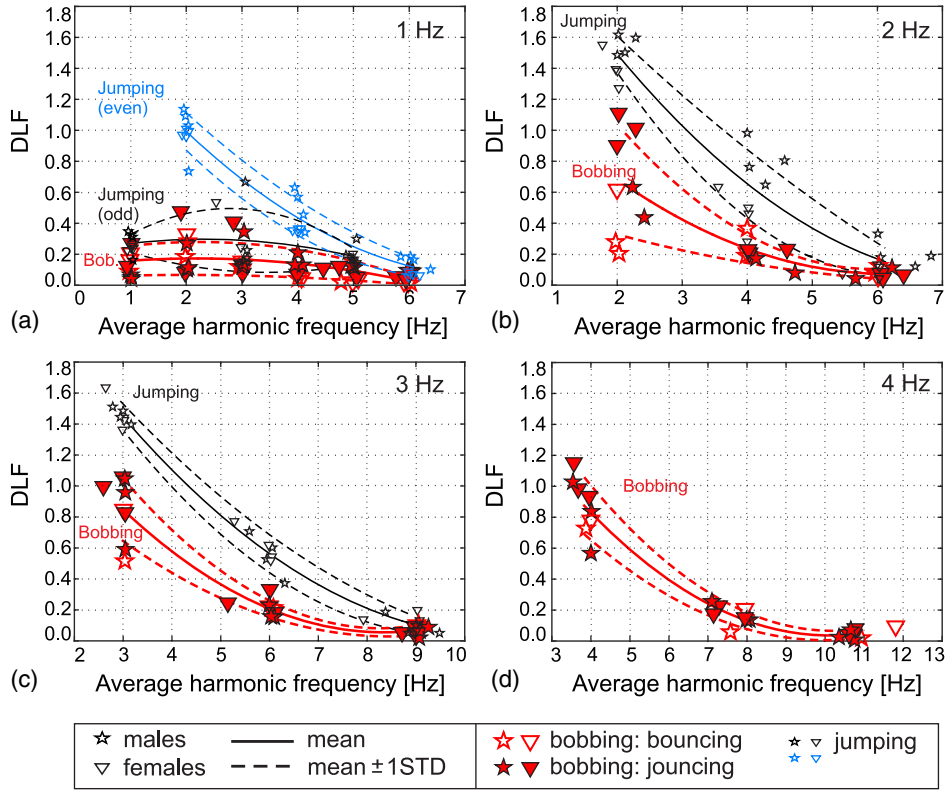

Fig. 6. DLFs (up to frequency of 6 Hz or third harmonic, whichever is larger) for jumping and/or bobbing at (a) 1 Hz; (b) 2 Hz; (c) 3 Hz; (d) 4 Hz

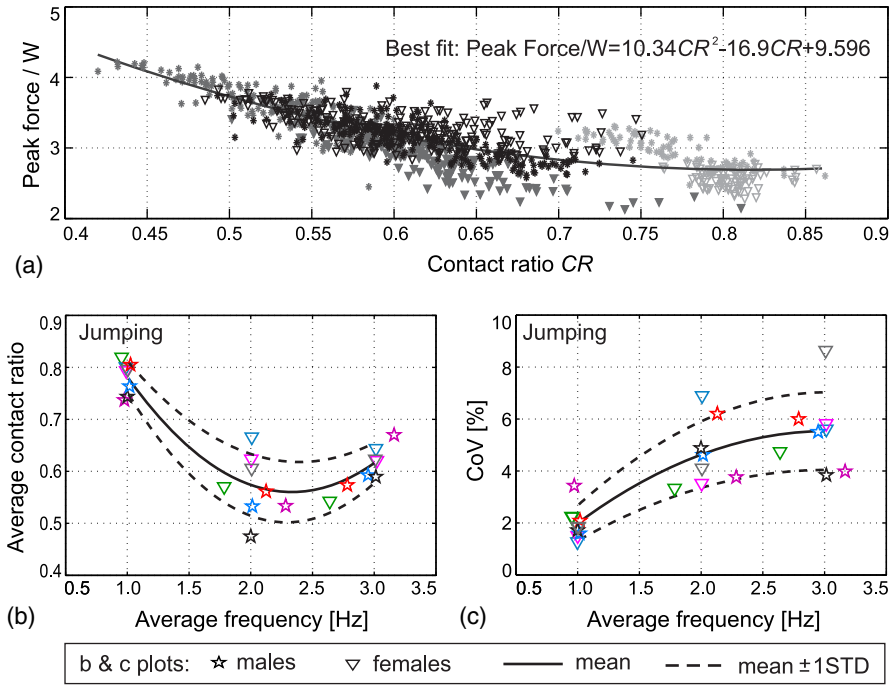

Fig. 7. (a) Weight-normalized peak force as a function of the contact ratio; light gray: 1 Hz, dark gray: 2 Hz, black symbols: 3 Hz; (b) average contact ratio; (c) its CoV as functions of the average frequency of jumping

The frequency of the SDOF system f_n is varied in steps of 0.1 Hz from 0.5 to 10 Hz. The lowest damping ratio that is realistically encountered in grandstand structures is around 1%, and it occurs in both steel-frame stands (e.g., Salyards and Hanagan 2007) and reinforced concrete structures [e.g., Manchester City stadium described in detail by Jones et al. (2011a)]. The lowest modal mass reported in literature is about 10,000 kg (Parkhouse and Ward 2010). These low, but feasible, values of damping ratio and modal

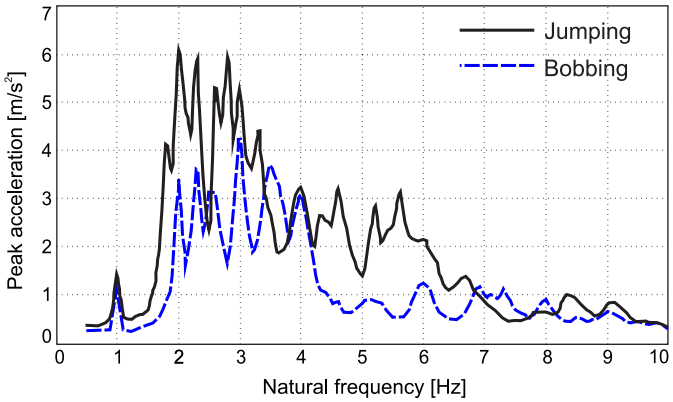

Fig. 8. Envelopes of peak acceleration response to jumping and bobbing

mass are chosen for the simulations as they represent structures that are expected to be most sensitive to small variations in the dynamic loading. In addition, the chosen value of the modal mass allows for quick calculation of the vibration response for structures having an arbitrary modal mass by simply multiplying the calculated response by a scaling factor (i.e., 10,000 divided by the actual modal mass).

Actual Acceleration of the Structure

The measured force was cut to an integer number of cycles and then extended by repeating itself to reach a duration of about 40 s. The force was then applied to the SDOF model of the structure to calculate the vibration response. The 40-s signal duration provides sufficient time to achieve a representative response time history. The Newmark numerical procedure (Chopra 1995) was used to solve the equation of motion.

An envelope of the peak response to the measured force while jumping is shown as a solid line in Fig. 8. The responses are dominated by the first forcing harmonics in the 2–3 Hz range and are about two times larger than the responses due to second harmonic (4–6 Hz frequency range). For bobbing (dashed line), the responses to the first harmonic (2–4 Hz) are occasionally more than three times larger than those from the second harmonic of the force (4–8 Hz). For the first two harmonics, the response to jumping is consistently larger than that from the bobbing action at the same frequency, in line with the DLF relationships observed in Fig. 6. An exception is at 1 Hz, where similar response values for both jumping and bobbing occur. The responses above 7 Hz (mainly due to the third harmonics) are similar for bobbing and jumping actions.

In addition to the extremely low modal mass of 10,000 kg (hereafter referred to as Case 1), the results will be discussed for a modal mass of about 35,000 kg (Case 2), which is more frequently encountered in practice. Some examples of the latter are two vibration modes of the Manchester City stadium (Jones et al. 2011a) and two grandstands described by Parkhouse and Ward (2010). Fig. 8 shows that the largest acceleration response to jumping is just above 6.0 m/s^2 for Case 1 and is about 1.7 m/s^2 (i.e., 3.5 times lower) for Case 2, while for bobbing it is 4.2 and 1.2 m/s^2, respectively. According to ISO (2007), humans are most sensitive to vibrations in the frequency range 4–8 Hz. In this frequency region the limiting (equivalent peak) vibration level for comfort on stadia is 1.4 m/s^2, while for safety (i.e., preventing panic) it is 2.8 m/s^2. The limits are less strict for frequencies below 4 Hz and above 8 Hz. For example, at 2 Hz, they reach 2.2 and 4.5 m/s^2, respectively. Fig. 8, therefore, demonstrates that a single person could cause vibrations that are mainly within the stated comfort level on a stand having modal mass of 35,000 kg, while the same activity on a stand of 10,000 kg could approach or even exceed the limit set for panic events. These calculations serve to illustrate excitation potential by a single person on an empty stand (a loading scenario that is more likely to occur before or after, rather than during, a sports or music event), and therefore the acceleration limit for panic events is used here to illustrate severity of the vibrations, rather than imply actual panic happening. The antinode of the vibration mode was assumed to be both the excitation and the response point in the simulations.

Influence of Cycle-by-Cycle Randomness on Vibration Response

Having characterized variability in the dynamic force and having an insight into the possible structural response level, it is interesting to determine how sensitive the vibration response is to the variability in the forcing parameters. The sensitivity is investigated for jumping activity in relation to the three parameters: peak force, frequency, and contact ratio.

The actual acceleration response to the measured forces has already been calculated in the previous section. To determine the significance of cycle-by-cycle variability in the force, three artificial force profiles have been created for each measured force. In each case, variability in one of the three parameters considered was removed from the force record:

1. Constant peak force: The average peak force was calculated for each time history, as explained in the "Peak Force" section. The forcing profile for each individual cycle was then scaled to enforce this value of the peak force;
2. Constant period (i.e., frequency): The average period (corresponding to the average frequency reported in the "Activity Frequency" section) was enforced on each cycle by applying appropriate scaling factor along the time axis, therefore stretching or compressing the force profile along this axis; and
3. Constant contact ratio: The average contact ratio from the "Contact Ratio for Jumping" section was enforced on each cycle by applying an appropriate scaling factor, while keeping the period unaltered.

In the latter two cases, the scaling along the time axis altered the original time step in the scaled sections of the force time history. To ensure equidistant time steps and preserve specific features of the newly formed time histories, the last two cases were resampled at 5,000 Hz using linear interpolation. The measured and the three artificially created force signals were then applied to all SDOFs analyzed in the previous section. The peak acceleration responses to the artificial forces were divided by the peak response to the measured forces to calculate the ratios shown in Fig. 9.

Fig. 9 reveals that the response is least sensitive to the randomness in the peak force [Fig. 9(a)], with almost all responses being within ±20% error boundaries. The sensitivity to the variability in the contact ratio is slightly higher [Fig. 9(c)], but still the majority of the responses exhibit an error up to ±20%. Finally, Fig. 9(b) shows that the response is most sensitive to variations in the frequency and that neglecting this type of variability could result in both under- and over-estimation of the actual response, with a factor of 2 being readily possible.

Results of this study suggest that the cycle-by-cycle variability in the activity frequency should be included in the force modeling in order to improve the accuracy in the response prediction. Neglecting this type of variability could result in an overestimation of the vibration response when the average pacing frequency coincides with the structural frequency, as well as underestimations of the out-of-resonance response, similar to findings concerned

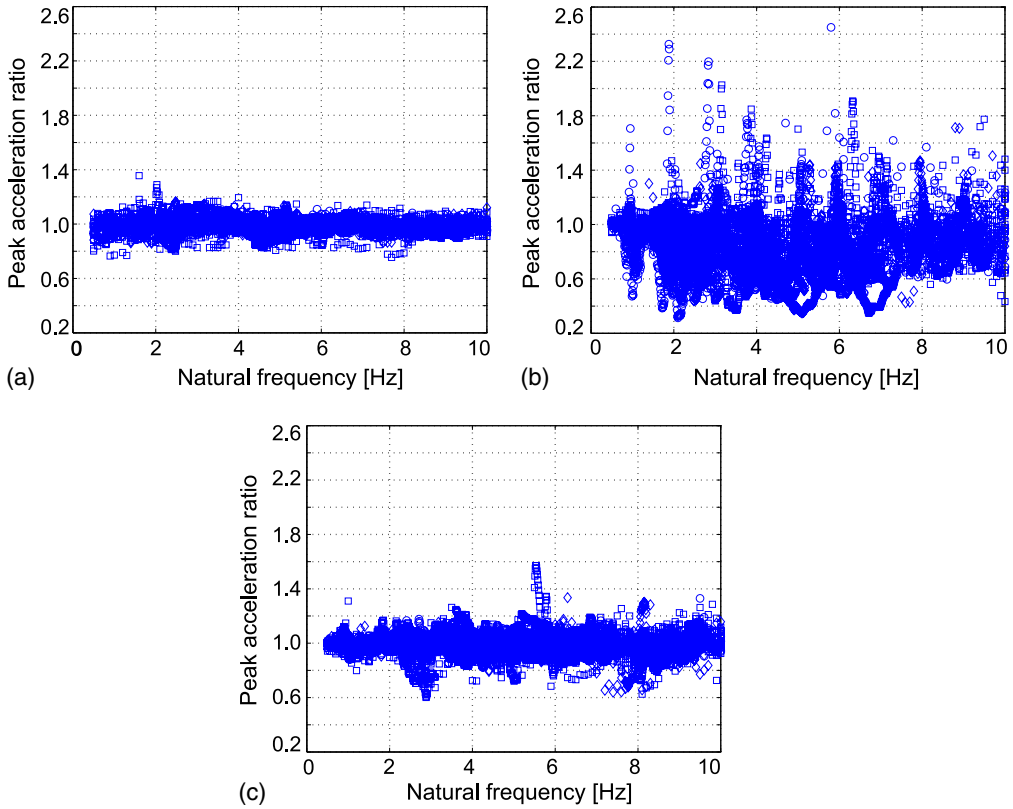

Fig. 9. Ratio between the peak acceleration responses to artificial and measured forces, with the artificial force having a constant: (a) peak force; (b) period; (c) contact ratio

with walking activity (Brownjohn et al. 2004; Van Nimmen et al. 2014).

The variations in the peak force and contact ratio are less influential. However, they still should be considered in response simulations to avoid an accumulation of errors in the response prediction, especially when the structure under analysis is on the verge of failing vibration serviceability requirements.

Ground Reaction Force

The vertical component of the time-domain acceleration signal for the ith marker, $a_i(t)$, was calculated by differentiating the measured displacement twice. The corresponding vertical component of the GRF, F_i (t), hereafter referred to as the indirect force, was then calculated by multiplying the test subject's mass by the net vertical acceleration

$$F_i(t) = m[a_i(t) - g] \tag{1}$$

where g = acceleration of gravity. The accuracy in measuring this force was then evaluated by comparing it with the benchmark force recorded using the force plate, hereafter referred to as the direct force.

The coefficient of determination R^2 (Draper and Smith 1985) was used to quantify how well the indirect force correlated with the direct force in the time domain. Then the influence of the measurement error on the structural response was evaluated.

Measuring Force Using the Kinematics of a Single Point

The average values of the R^2 coefficients, across the population of eight test subjects, are calculated for all 17 markers and for each activity frequency. The mean and SD values for each marker across all tests are also found. The results are presented in Table 3 for both jumping and bobbing activities.

It can be seen that the markers in the hip and back groups perform noticeably better than the front markers. This is expected given that the front markers are most prone to soft tissue artefacts. Table 3 reveals that marker B6 performed best across all frequencies and for both activities. Higher force accuracy was achieved for jumping. The same conclusion was reached when comparing the forces in the frequency domain (McDonald 2015).

The quality of the force measured using the B6 marker is shown in Fig. 10 for two trials. Figs. 10(a and b) demonstrate an excellent agreement, in both the time domain and frequency domains, between the indirectly and directly measured forces for a 2-Hz jumping trial. Figs. 10(c and d) show an example of poorer agreement for a 4-Hz bobbing trial, where overestimation of both the second and third harmonics can be seen.

Error in Indirectly Measured Force

The indirectly measured force contains errors from several sources: measurement error of the motion capture system, error due to the assumption that a single point on the body surface has the same kinematics as the body centre of mass, and error due to soft tissue artefacts. While it is known that the first error is small (up to 1 mm in measured displacement trajectories), the other two errors are not possible to evaluate individually. What is of interest in this study is

Table 3. R^2 Values for the Three Groups of Markers (H = Hip, F = Front, and B = Back)

	R^2 for jumping					R^2 for bobbing					
Marker	1 Hz	2 Hz	3 Hz	Mean	SD	1 Hz	2 Hz	3 Hz	4 Hz	Mean	SD
RH1	0.969	0.970	0.921	0.953	0.023	0.924	0.947	0.905	0.775	0.888	0.110
RH2	0.963	0.963	0.904	0.943	0.028	0.907	0.928	0.891	0.727	0.863	0.129
LH2	0.955	0.956	0.895	0.935	0.028	0.908	0.938	0.891	0.724	0.865	0.126
LH1	0.965	0.966	0.911	0.947	0.026	0.930	0.954	0.920	0.772	0.894	0.119
F1	0.911	0.920	0.824	0.885	0.043	0.922	0.916	0.788	0.598	0.816	0.180
F2	0.885	0.900	0.789	0.858	0.049	0.888	0.880	0.696	0.577	0.768	0.187
F3	0.838	0.837	0.684	0.786	0.072	0.786	0.819	0.592	0.553	0.698	0.218
F4	0.834	0.842	0.720	0.799	0.056	0.788	0.816	0.567	0.458	0.674	0.233
F5	0.830	0.841	0.722	0.798	0.054	0.795	0.813	0.574	0.449	0.668	0.241
F6	0.821	0.832	0.749	0.801	0.037	0.736	0.809	0.630	0.482	0.670	0.242
F7	0.877	0.902	0.822	0.867	0.033	0.819	0.865	0.776	0.749	0.804	0.160
B1	0.911	0.935	0.777	0.874	0.070	0.887	0.893	0.776	0.565	0.788	0.204
B2	0.939	0.953	0.843	0.912	0.049	0.880	0.891	0.827	0.505	0.776	0.201
B3	0.955	0.966	0.857	0.926	0.049	0.916	0.926	0.842	0.536	0.805	0.199
B4	0.968	0.975	0.923	0.956	0.023	0.930	0.962	0.922	0.790	0.901	0.087
B5	0.969	0.973	0.934	0.959	0.017	0.915	0.951	0.919	0.866	0.913	0.065
B6	0.971	0.979	0.950	0.967	0.012	0.924	0.960	0.929	0.902	0.929	0.062

Note: L and R denote left and right, respectively.

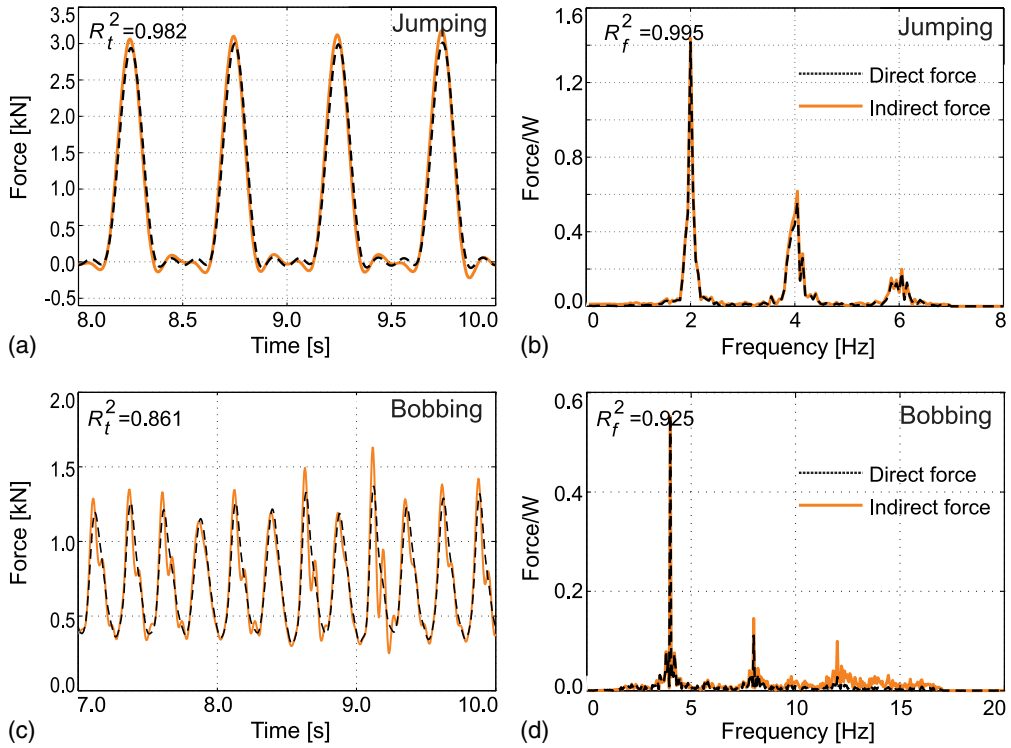

Fig. 10. Comparison between the directly measured (dashed line) and indirectly measured force using the B6 marker (solid line) in (a) time domain; (b) frequency domain for jumping at 2 Hz; (c) time domain; (d) frequency-domain for bobbing at 4 Hz

evaluation of the success of the indirect force measurement by gaining an insight into the accumulated (total) error. To achieve this, the acceleration response to the force measured using the B6 maker is calculated for the SDOF systems using a damping ratio of 1% and natural frequency values in the 0.5–7.0 Hz range. The ratio r_A between the peak vibration response to the indirectly measured force A_{indirect} and the peak response to the directly measured force A_{direct} is calculated

$$r_A = \frac{A_{indirect}}{A_{direct}} \tag{2}$$

where $r_A > 1$ indicates that the indirect force results in an overestimation of the structural response, whereas $r_A < 1$ relates to an underestimation of the actual response.

The response ratio as a function of the natural frequency of the structure for jumping at 1, 2, and 3 Hz is shown in Fig. 11.

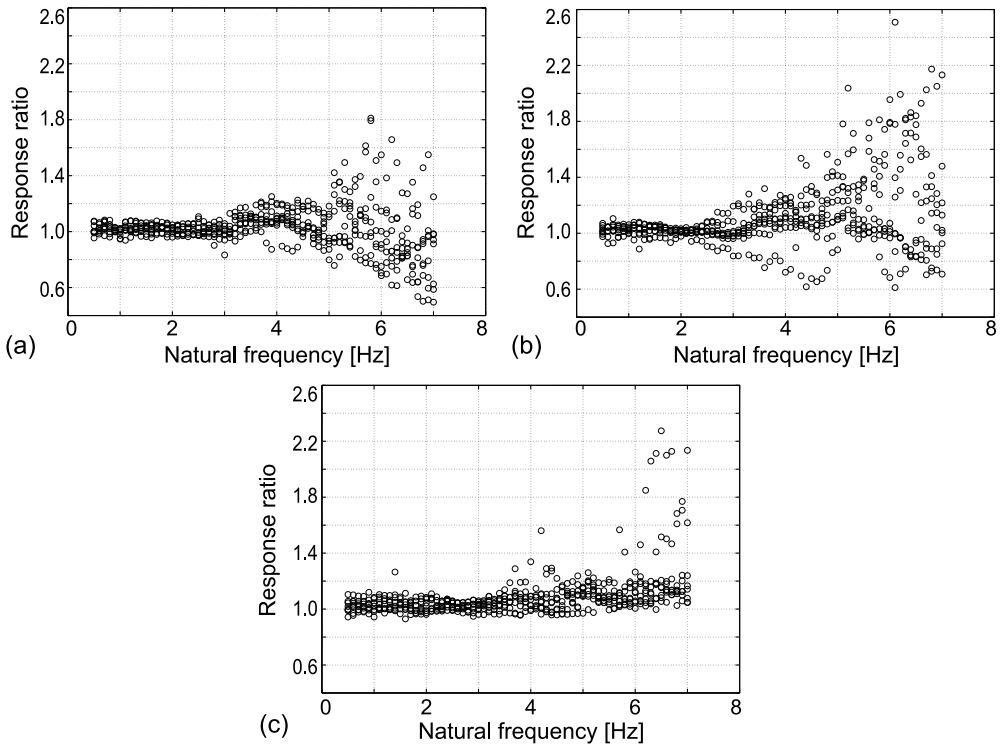

Fig. 11. Response ratio r_A as a function of the natural frequency of the structure for jumping at (a) 1 Hz; (b) 2 Hz; (c) 3 Hz

The response ratio is between 0.8 and 1.2 for natural frequencies $f_n \leq 3$ Hz, for jumping at 1 Hz [Fig. 11(a)]. Therefore, the structural response to first three harmonics of the force is within a $\pm 20\%$ error band. In fact, the error is outside this band only occasionally even at the higher frequency range of 3–5 Hz. At and around the natural frequency of 6 Hz, the error in the indirect force is much larger, with the response ratio ranging from 0.4 to 1.8.

For jumping at 2 Hz [Fig. 11(b)], the response is largely within $\pm 20\%$ error band for $f_n \leq 4$ Hz, suggesting that the first two harmonics of the indirect force are reasonably good representations of the actual dynamic excitation. At and around 6 Hz, the error increases significantly, with the ratio ranging from 0.6 to 2.5. Finally, the response ratio to jumping at 3 Hz is largely within $\pm 20\%$ error band for $f_n \leq 6$ Hz [Fig. 11(c)].

It can be concluded that the accuracy of the force measurement using the B6 marker is excellent for force components that excite structures with $f_n \leq 3$ Hz. This includes the first three harmonics for jumping at 1 Hz and the first harmonic for jumping at 2 and 3 Hz. For structures with a natural frequency between 3 and 5 Hz, the accuracy decreases; however, the response prediction is still largely within the $\pm 20\%$ error. Finally, for structures with a natural frequency between 5 and 7 Hz, the response error becomes substantial, for all but jumping at the fastest rate of 3 Hz.

Therefore, using the force derived from the kinematics of the B6 marker results in a very good estimate of the first harmonic of the dynamic force for all frequencies, and adequate estimate of the second harmonic of the force. The error becomes large for the third harmonic (apart from jumping/bobbing at 1 Hz). These results suggest that using the B6 marker to capture the frequency content of the force up to 5 Hz is acceptable.

Fig. 12 shows the response ratio information for bobbing. A greater spread of r_A values in Fig. 12 suggests that the error in force measurement while bobbing is greater than while jumping at nominally the same frequencies. However, the error in the response for structures with a natural frequency up to 4 Hz (which normally exhibit the largest response to bobbing, Fig. 8) is still contained within 20% error in 92% of trials (McDonald 2015). For structural frequencies above 4 Hz, the response ratio can be as low as 0.6, underestimating the actual structural response, and as large as 3, significantly overestimating the actual response. Therefore, using the kinematics of the B6 marker to derive the bobbing force results in good estimates of the first four harmonics for bobbing at 1 Hz, the first two harmonics for bobbing at 2 Hz, and the first harmonic when bobbing at higher frequencies.

Discussion and Conclusions

Summary of Experiments

The GRFs for eight test subjects jumping and bobbing in the Gait Laboratory at the University of Warwick were recorded using a force plate. In parallel, kinematics of the body was monitored using a motion capture system. Jumping was performed with the aid of a metronome at three frequencies: 1, 2, and 3 Hz, while bobbing included an additional frequency of 4 Hz. The peak force and the frequency of the GRF profiles, as well as the peak to peak displacement of the human body, were extracted on a cycle-by-cycle basis for the two activities. In addition the contact ratios were extracted for the jumping trials. The DLFs were calculated for at least three harmonics of the measured forces.

Displacement of Trunk

The peak to peak displacement of the trunk while jumping was 15–25 cm at the slowest frequency of 1 Hz and around 8 cm at the fastest frequency of 3 Hz. For bobbing the displacements were 2–15 cm at 1 Hz and 2–3 cm at 4 Hz. Larger jumping displacements are expected due to the more energetic nature of this activity.

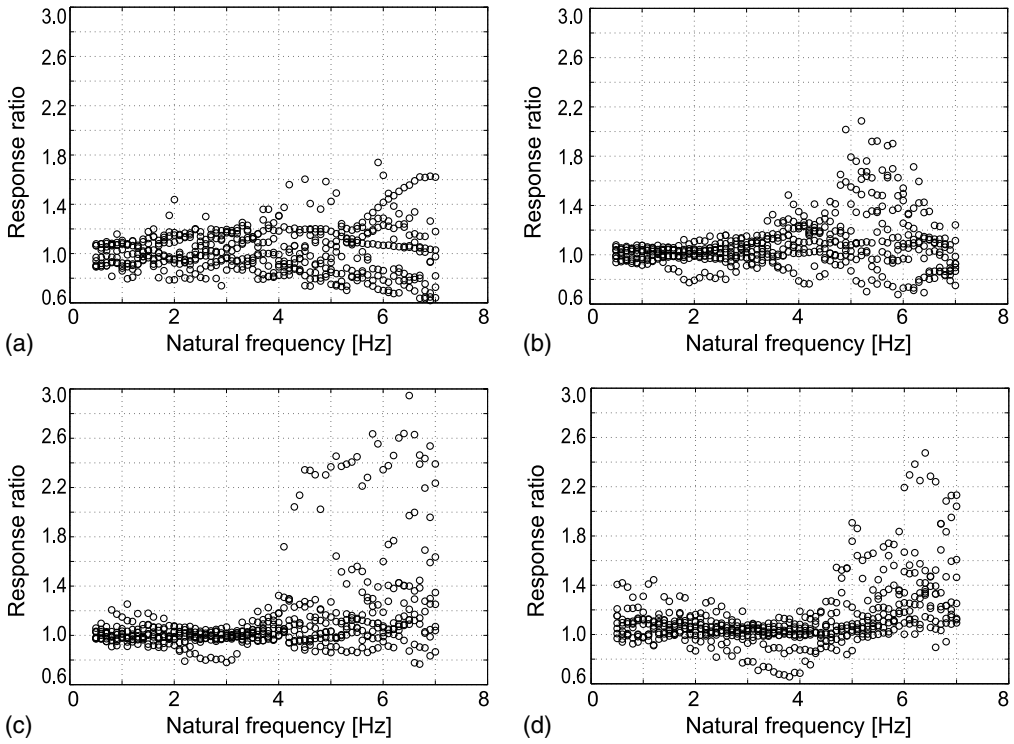

Fig. 12. Response ratio r_A as a function of the natural frequency of the structure for bobbing at (a) 1 Hz; (b) 2 Hz; (c) 3 Hz; (d) 4 Hz

The intersubject variability in the displacement while bobbing is much larger, especially for lower frequencies [Fig. 4(c)]. The cycle-by-cycle variations, on the other hand, range between 4 and 16% for jumping and between 5 and 30% for bobbing, suggesting that consistent bobbing is more difficult than jumping.

Ground Reaction Force

The movement of the human body generates the dynamic GRF, and it is expected that the more energetic activity of jumping results in the largest forces. This is confirmed in the present study: the peak force ranges between 2.5 and 4.0 times the body weight for jumping, compared with 1.3–2.5 times the body weight while bobbing. In both cases the intersubject variations are significant; especially at the midfrequency range [Figs. 5(a and c)]. The cycle-by-cycle variations are again larger for bobbing (3–11%) compared with jumping (3–7%, with one trial reaching an atypical value of 10%).

DLFs are functions of the frequency of the activity (Fig. 6), however only the maximum values achieved in the experiments will be quoted here and only for frequencies that are more likely in practice (i.e., frequencies above 1 Hz). For jumping, these values go are up to 1.7 for the first harmonic, up to 1.0 for the second and up to 0.35 for the third. The equivalent values for bobbing are 1.1, 0.4, and 0.1, respectively. While larger DLFs for jumping are in line with previous findings on the body kinematics and peak forces, it is interesting that the differences in DLFs are more pronounced at higher harmonics. Overall, bobbing DLFs are around two times lower than those induced by jumping, but greater than the DLFs for walking (Dang and Živanović 2015).

Variability in Activity Frequency

The study shows that cycle-by-cycle variation in the activity frequency ranges mainly between 2 and 6% for both jumping and bobbing. Only one trial exceeded this range for jumping (8%), and three trials (6.5, 9, and 10.5%) exceeded it for bobbing. However, on average the variability is larger for bobbing, which is in line with the findings for the other parameters analyzed. The variability in jumping and bobbing is therefore more than two times greater than when walking at a normal speed (Dang and Živanović 2015). Despite this fact, modeling the randomness in the walking force is more frequently studied and better developed than for jumping and bobbing activities.

Variability in Contact Ratio

The contact ratios for jumping activity were found to vary between values of 0.45 and 0.82, suggesting that the old BS 6399 specification of 0.25–0.67 underestimated the actual range, resulting in a shorter duration of the force and a potentially overconservative force model. These recommendations have since been removed from the standard (BSI 2010), emphasizing the need for further research and development of force models. Finally, the jump-by-jump variations in the contact ratio range from low values of 1–3% at 1 Hz to larger variations of 4–9% at 3 Hz.

Sensitivity of Vibration Response to Force Variability

Stated variations in the force parameters can be used in the structural design phase to investigate the sensitivity of the vibration response to human actions. Such a sensitivity study has been performed for jumping in this paper. It has been shown that the response is most sensitive to cycle-by-cycle variations in the activity frequency. Neglecting this type of variation could lead to both underestimations (by up to 70%) and overestimations (by up to 140%) of the actual response [Fig. 9(b)]. Given that the bobbing forces were found to generally exhibit larger cycle-by-cycle variation compared to jumping, the importance of modeling the force variability is even greater in this case. The variations in the peak force and contact ratio influenced the vibration response to a lesser degree, but they still should be considered in modeling to avoid an accumulation of errors in the response prediction.

Best Location on Human Body for Measuring Force

To monitor body kinematics, 17 points on the human body were tracked using a motion capture system; 13 markers were systematically attached to the trunk of the test subject, while the remaining four markers were attached to the hips. The ultimate aim was to identify the points that best represent the BCoM kinematics and the resulting GRF. It was found that monitoring the C7th vertebrae at the base of the neck was suitable for accurate measurement of the frequency content of the force up to 5 Hz for jumping and up to 4 Hz for bobbing activity.

Utilizing C7 in Future Research

The proposed simplified measurement method has potential to be used for monitoring of groups and crowds during sports and music events. However the use of the motion capture system currently limits the method to mostly laboratory environments. Further research may facilitate the monitoring of the C7th vertebrae in situ by using markerless video recording—a methodology that has already been successfully explored for monitoring body kinematics by tracking head movement (Hoath et al. 2007). Alternatively, utilizing wireless technologies, such as those consisting of inertial (Van Nimmen et al. 2014) and magnetometer sensors could be employed. The latter application would be limited to studies with prerecruited participants due to the need to instrument them with wireless devices. Regardless of this limitation, both (video and wireless) approaches could prove to be extremely valuable for data collection on as-built structures.

Monitoring of the C7th vertebrae could be used not only in future measurements of the low-frequency content of the force and the intrasubject variations in the key parameters, but also for observing human–human interaction (e.g., potential for synchronization). These measurements are of particular interest for jumping and bobbing on slender, perceptibly oscillating (i.e., nonrigid) structures. It is known that humans jumping and bobbing in groups interact with each other as well as with oscillating structures and that there is a need for event-based evaluation of the structural vibration response that could accurately account for these interactions (Yao et al. 2004, 2006; Parkhouse and Ward 2010; Jones et al. 2011a; Catbas et al. 2010; Salyards and Hua 2015). However, detailed insights into the influence of structural vibration on the actual kinematics of humans bobbing and jumping and into human–human interactions within groups and crowds are not available. This paper identifies body location suitable for monitoring and characterizes the variability of jumping and bobbing activities on rigid surfaces. These outputs are expected to inform measurements on in situ structures, to be used as a benchmark for evaluating the potential influence of structural vibration on human jumping and bobbing actions and to facilitate development of stochastic loading models in future research.

Data Availability

Electronic format of the data collected in this research can be downloaded free of charge from the University of Warwick webpage http://wrap.warwick.ac.uk/80470/.

Acknowledgments

This research work was partly supported by the U.K. Engineering and Physical Sciences Research Council (EPSRC) [grant number EP/I03839X/1: *Pedestrian Interaction with Lively Low-Frequency Structures*]. The first author was supported by EPSRC DTG Scholarship. The authors would like to thank Birmingham Science City and Advantage West Midlands for the access to the Gait Laboratory.

References

AMTI (Advanced Mechanical Technology). (2007). "Force plate manual—Model OR6-7." Watertown, MA.

Bachmann, H., and Ammann, W. (1987). "Vibrations in structures: Induced by man and machines." International Association for Bridge and Structural Engineering, Zurich, Switzerland.

BRE (Building Research Establishment). (2004). "The response of structures to dynamic crowd loads." Watford.

Brownjohn, J. M. W., Pavic, A., and Omenzetter, P. (2004). "A spectral density approach for modelling continuous vertical forces on pedestrian structures due to walking." *Can. J. Civ. Eng.*, 31(1), 65–77.

BSI (British Standards Institution). (2002). "1996 loading for buildings—Part 1: Code of practice for dead and imposed loads dead and imposed loads." *BS 6399-1*, London.

BSI (British Standards Institution). (2010). "Eurocode 1: Actions on structures—Part 1-1: General actions—Densities, self-weight, imposed loads for buildings." *BS EN 1991-1-1:2002*, London.

Catbas, F. N., Gul, M., and Sazak, H. O. (2010). "Dynamic testing and analysis of a football stadium." *28th Proc., IMAC*, The Printing House, Stoughton, WI.

Chopra, A. K. (1995). *Dynamics of structures*, Prentice-Hall, NJ.

Dang, H. V., and Živanović, S. (2015). "Experimental characterisation of walking locomotion on rigid level surfaces using motion capture system." *Eng. Struct.*, 91(15), 141–154.

Dougill, J. W., Wright, J. R., Parkhouse, J. G., and Harrison, R. E. (2006). "Human structure interaction during rhythmic bobbing." *Struct. Eng.*, 84(22), 32–39.

Draper, N., and Smith, H. (1985). *Applied regression analysis*, Wiley, New York.

Ellis, B. R., and Ji, T. (1994). "Floor vibrations induced by dance-type loads: Verification." *Struct. Eng.*, 72(3), 45–50.

Ginty, D., Derwent, J. M., and Ji, T. (2001). "The frequency ranges of dance-type loads." *Struct. Eng.*, 79(6), 27–31.

Hoath, R. M., Blakeborough, A., and Williams, M. S. (2007). "Using video tracking to estimate the loads applied to grandstands by large crowds." *25th IMAC*, The Printing House, Stoughton, WI.

ISO (International Organization for Standardization). (2007). "Bases for design of structures—Serviceability of buildings and walkways against vibration." *ISO 10137*, Geneva.

IStructE (Institution of Structural Engineers). (2008). "Dynamic performance requirements for permanent grandstands subject to crowd action: Recommendations for management, design and assessment." Dept. for Communities and Local Government and Dept. for Culture Media and Sport, London.

Jones, C. A., Pavic, A., Reynolds, P., and Harrison, R. E. (2011a). "Verification of equivalent mass-spring-damper models for crowd-structure vibration response prediction." *Can. J. Civ. Eng.*, 38(10), 1122–1135.

Jones, C. A., Reynolds, P., and Pavic, A. (2011b). "Vibration serviceability of stadia structures subjected to dynamic crowd loads: A literature review." *J. Sound Vib.*, 330(8), 1531–1566.

MATLAB version 7.13.0.564 [Computer software]. MathWorks, Natick, MA.

McDonald, M. G. (2015). "Experimental characterisation of jumping and bobbing actions for individuals and small groups." Ph.D. thesis, School of Engineering, Univ. of Warwick, Coventry, U.K.

Nexus version 1.4.1. [Computer software]. Oxford Metrics Group, Oxford, U.K.

Parkhouse, G., and Ward, I. (2010). "Design charts for the assessment of grandstands subject to dynamic crowd action." *Struct. Eng.*, 88(7), 27–34.

Pernica, G. (1990). "Dynamic load factors for pedestrian movements and rhythmic exercises." *Can. Acoust.*, 18(2), 3–18.

Racic, V., Brownjohn, J. M. W., Wang, S., Elliot, M. T., and Wing, A. (2013a). "Effect of sensory stimuli on dynamic loading induced by people bouncing." *31st IMAC*, Springer, New York.
Racic, V., and Chen, J. (2015). "Data-driven generator of stochastic dynamic loading due to people bouncing." *Comput. Struct.*, 158(1), 240–250.
Racic, V., and Pavic, A. (2010a). "Mathematical model to generate near-periodic human jumping force signals." *Mech. Syst. Signal Process.*, 24(1), 138–152.
Racic, V., and Pavic, A. (2010b). "Stochastic approach to modelling of near-periodic jumping loads." *Mech. Syst. Signal Process.*, 24(8), 3037–3059.
Racic, V., Pavic, A., and Brownjohn, J. M. W. (2013b). "Modern facilities for experimental measurement of dynamic loads induced by humans: A literature review." *Shock Vib.*, 20(1), 53–67.
Rainer, J. H., Pernica, G., and Allen, D. E. (1988). "Dynamic loading and response of footbridges." *Can. J. Civ. Eng.*, 15(1), 66–71.
Salyards, K. A., and Hanagan, L. M. (2007). "Analysis of coordinated crowd vibration levels in a stadium structure." *25th Proc., IMAC*, The Printing House, Stoughton, WI.
Salyards, K. A., and Hua, Y. (2015). "Assessment of dynamic properties of a crowd model for human-structure interaction modelling." *Eng. Struct.*, 89(15), 103–110.
Sim, J. H., Blakeborough, A., and Williams, M. S. (2005). "Dynamic loads due to rhythmic jumping and bobbing." *Structural Dynamics: EURODYN 2005*, Paris.
Sim, J. H., Blakeborough, A., Williams, M. S., and Parkhouse, J. G. (2008). "Statistical model of crowd jumping loads." *J. Struct. Eng.*, 10.1061/(ASCE)0733-9445(2008)134:12(1852), 1852–1861.
Thorton-Trump, A. B., and Daher, R. (1975). "The prediction of the reaction forces from gait data." *J. Biomech.*, 8(3–4), 173–178.
Van Nimmen, K., Lombaert, G., Jonkers, I., De Roeck, G., and Van den Broeck, P. (2014). "Characterisation of walking loads by 3D inertial motion tracking." *J. Sound Vib.*, 333(20), 5212–5226.
Yao, S., Wright, J. R., Pavic, A., and Reynolds, P. (2002). "Forces generated when bouncing or jumping on a flexible structure." *ISMA Int. Conf. on Noise and Vibration Engineering*, Katholieke Universiteit Leuven, Leuven, Belgium.
Yao, S., Wright, J. R., Pavic, A., and Reynolds, P. (2004). "Experimental study of human-induced dynamic forces due to bouncing on a perceptibly moving structure." *Can. J. Civ. Eng.*, 31(6), 1109–1118.
Yao, S., Wright, J. R., Pavic, A., and Reynolds, P. (2006). "Experimental study of human-induced dynamic forces due to jumping on a perceptibly moving structure." *J. Sound Vib.*, 296(1–2), 150–165.